Fluorescence of fluorescein attached to myosin SH1 distinguishes the rigor state from the actin-myosin-nucleotide state

ARTICLE *in* BIOCHEMISTRY · FEBRUARY 1984

Impact Factor: 3.02 · DOI: 10.1021/bi00297a029 · Source: PubMed

1 AUTHOR:

Toshio Ando
Kanazawa University
130 PUBLICATIONS **3,964** CITATIONS

Heatley, F., Scott, J. E., Jeanloz, R. W., & Walker-Nasir, E. (1982) *Carbohydr. Res. 99*, 1-11.
Highsmith, S., Garvin, J. H., Jr., & Chipman, D. M. (1975) *J. Biol. Chem. 250*, 7473-7480.
Hoffman, P., Meyer, K., & Linker, A. (1956) *J. Biol. Chem. 219*, 653-663.
Kantor, T. G., & Shubert, M. (1956) *J. Am. Chem. Soc. 79*, 152-153.
Kim, J. J., & Conrad, H. E. (1974) *J. Biol. Chem. 249*, 3091-3097.
Kim, J. J., & Conrad, H. E. (1976) *J. Biol. Chem. 251*, 6210-6217.
Kim, J. J., & Conrad, H. E. (1977) *J. Biol. Chem. 252*, 8292-8299.
Kim, J. J., & Conrad, H. E. (1980) *J. Biol. Chem. 255*, 1586-1597.
Kim, J. J., & Conrad, H. E. (1982) *J. Biol. Chem. 257*, 1670-1675.
Knudson, W. (1982) Ph.D. Thesis, University of Illinois, Urbana, IL.
Laskey, R. A., & Mills, A. D. (1975) *Eur. J. Biochem. 56*, 335-341.
Mathews, M. B. (1961) *Biochim. Biophys. Acta 48*, 402-403.
Maxam, A. M., & Gilbert, W. (1977) *Proc. Natl. Acad. Sci. U.S.A. 74*, 560-564.
Meyer, K. (1947) *Physiol. Rev. 27*, 335-340.
Meyer, K. (1971) *Enzymes, 3rd Ed. 5*, 307-320.
Meyer, K., & Rapport, M. M. (1952) *Adv. Enzymol. Relat. Areas Mol. Biol. 13*, 199-236.
Meyer, K., Hoffman, P., & Linker, A. (1960) *Enzymes, 2nd Ed. 4*, 447-460.
Michelacci, Y. M., & Dietrich, C. P. (1976) *Biochim. Biophys. Acta 451*, 436-443.
Morris, E. R., Rees, D. A., & Welsh, E. J. (1980) *J. Mol. Biol. 138*, 383-400.
Rees, D. A. (1975) *Int. Rev. Sci.: Biochem., Ser. One 5*, 1-42.
Saito, H., Yamagata, T., & Suzuki, S. (1968) *J. Biol. Chem. 243*, 1536-1542.
Scott, J. E., & Tigwell, M. J. (1978) *Biochem. J. 173*, 103-114.
Scott, J. E., & Heatley, F. (1979) *Biochem. J. 181*, 445-449.
Scott, J. E., Heatley, F., Moorcroft, D., & Olavesen, A. H. (1981) *Biochem. J. 199*, 829-832.
Seno, N., Anno, K., Yaegashi, Y., & Okuyama, T. (1975) *Connect. Tissue Res. 3*, 87-96.
Weissmann, B. (1955) *J. Biol. Chem. 216*, 783-794.
Welti, D., Rees, D. A., & Welsh, E. J. (1979) *Eur. J. Biochem. 94*, 505-514.
Zaneveld, L. J. D., Polakoski, K. L., & Schumacher, G. F. B. (1973) *J. Biol. Chem. 248*, 564-570.

Fluorescence of Fluorescein Attached to Myosin SH_1 Distinguishes the Rigor State from the Actin-Myosin-Nucleotide State†

Toshio Ando

ABSTRACT: It has been found that the fluorescence intensity of 5-(iodoacetamido)fluorescein (5-IAF) attached to the SH_1 of myosin subfragment 1 (S-1) increases 3-fold on formation of the rigor complex. On adding Mg^{2+}-ADP, light scattering indicates no dissociation, but the fluorescence increment disappears. Thus, this fluorescence signal can distinguish the rigor state from other states, especially from ternary complexes such as actin-myosin-nucleotide. We demonstrate that by using this signal we can measure spectroscopically several kinetic parameters of acto-S-1-nucleotide interaction: In the presence of 20 mM KCl, 2 mM $MgSO_4$, and 10 mM TES (pH 7.5) at 22 °C, Mg^{2+}-ADP binds to acto-S-1_5* (S-1_5* denotes 5-IAF-labeled S-1) with a $K_a = 2 \times 10^6$ M^{-1}, and Mg^{2+}-PP_i binds to acto-S-1_5* with two apparent affinities, $K_a = 8 \times 10^4$ M^{-1} and 1.4×10^3 M^{-1}; the association rates of Mg^{2+}-ADP and Mg^{2+}-ATP for acto-S-1_5* are 10^7 s^{-1} M^{-1} and 4×10^6 s^{-1} M^{-1}, respectively, and the dissociation rate of Mg^{2+}-ADP for acto-S-1_5* is 5 s^{-1}. In contrast to the fluorescence intensity of the dye, the lifetime and the absorbance are essentially unaffected by complex formation with F-actin or nucleotides. Therefore, we conclude that there must be a static quencher such as Trp, Tyr, or Met in the neighborhood of the attached dye and that the contact between dye and quencher is modulated by actin-induced or nucleotide-induced conformational changes in S-1.

Since muscle contraction is brought about by the cyclic interaction of actin-myosin-ATP, it is quite important to have fast indicators sensitive to intermediate states of this interaction. If the responses of such indicators (chemical signal) are available, we can apply them in vivo and try to correlate the chemical states of myosin cross-bridges with a physiological parameter such as tension or with a microscopic parameter such as cross-bridge inclination. Especially, we can then study such correlations in the time domain and deduce kinetic parameters (Morales, 1982). Although tension transients induced by quick stretch or release of isometrically contracting fibers have been studied (Huxley & Simmons, 1971, 1973), no one has yet tried to see directly and simultaneously the transients of chemical states along with the tension transients. Recently, a new type of fiber transient has been introduced by Goldman et al. (1982), by employment of flash photolysis of "caged ATP". The tension transient following quick conversion of caged ATP into ATP has been observed in the absence and presence of Ca^{2+}. But direct observation of chemical states of myosin cross-bridges was not made in that study. Rotational motion of myosin cross-bridges has been studied by analyzing

† From the Cardiovascular Research Institute, School of Medicine, University of California, San Francisco, California 94143. *Received July 11, 1983.* This research has been supported by Grants NSF PCM 75-22698 and NHBLI-16683.

0006-2960/84/0423-0375$01.50/0

fluctuations in fluorescence polarization of rhodamine-labeled cross-bridges in isometrically contracting fibers (Borejdo et al., 1979). But, again, fluctuations in the concentration of enzymatic intermediate states were not measured in order to cross correlate them with those in fluorescence polarization. Having in mind such experiments, we have been searching for the required chemical signals. We have recently reported that the binding of 1,N^6-ethenoadenosine 5′-triphosphate (ε-ATP)[1] can be made to give a very large fluorescence signal if the fluorescence of free ε-ATP in the bulk solution is being quenched by acrylamide (Ando et al., 1982a,b). This signal thus detects myosin–nucleotide binding.

The signal being reported here is a new chemical signal sensitive to other ATPase steps, viz., to actin–myosin binding and to nucleotide binding to acto–myosin. To obtain this signal, 5-IAF is specifically attached to the SH_1 of S-1. The fluorescence intensity of the fluorescein-labeled acto–S-1 is 3 times greater than that of fluorescein-labeled S-1, S-1–nucleotides, and acto–S-1–nucleotides. It is especially important that this signal can sensitively distinguish the rigor state from the ternary complex state, suggesting that S-1 conformation is different between the two actin-bound states. We demonstrate here how this signal can be used in obtaining kinetic parameters of the acto–S-1–nucleotide interaction. We also studied the mechanism of the fluorescence change and conclude that in the neighborhood of the attached dye there is a quencher of fluorescence [Trp, Tyr, and Met are known to be able to quench fluorescence of fluorescein (Watt & Voss, 1977)] and that the attached dye is in two states, one in which the dye is in contact with the quencher and one in which the dye is not in contact with the quencher. The equilibrium between the two states is shifted to the noncontact state by an actin-induced conformational change in S-1, resulting in the increase of the fluorescence intensity but in no change of the lifetime and the absorbance.

Materials and Methods

Muscle Protein Preparation. Myosin was prepared from rabbit skeletal muscle by the method of Tonomura et al. (1966). S-1 was obtained by digesting myosin with α-chymotrypsin (Sigma Chemical Co.) according to Weeds & Taylor (1975). S-1(A1) and S-1(A2) were not separated. Acetone powder was prepared from rabbit skeletal muscle as in Ando & Asai (1979). Actin was obtained from the acetone powder by the method of Spudich & Watt (1971). F-Actin (ca. 13 mg/mL) was stored in 0.2 mM ATP plus buffer A [20 mM KCl, 2 mM $MgSO_4$, and 10 mM TES (pH 7.5)] at 0 °C. Just before F-actin was used for experiments, the stored F-actin was centrifuged in a No. 50 rotor at 45K rpm for 20–30 min to remove free ATP, and the pellet was homogenized in buffer A. The cycle of centrifugation–homogenization was repeated twice, and finally, unhomogenized particles of F-actin were removed by a low-speed centrifugation. The molar concentration of S-1 was estimated from use of $E^{1\%}_{280} = 7.7$ and a molecular weight of 1.15×10^5, with correction for the tubidity ($1.93 \times$ the 330-nm absorbance was subtracted from the 280-nm absorbance). The molar concentration of F-actin was estimated from use of $E^{1\%}_{290} = 6.7$ and a molecular weight of 4.2×10^4 ($1.68 \times$ the 330-nm absorbance was subtracted from the 290-nm absorbance to correct for turbidity artifacts).

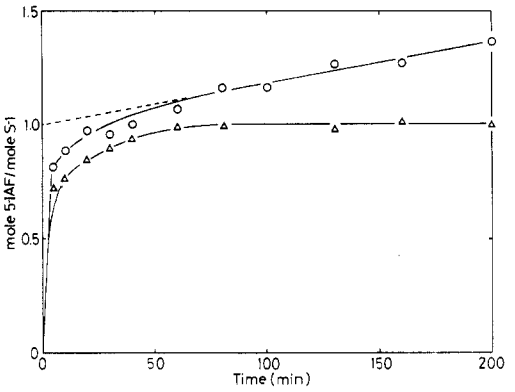

FIGURE 1: Time course of reaction of 5-IAF with S-1. S-1 is incubated with a 5-fold molar excess of the dye over S-1; then as a function of time, aliquots are withdrawn and passed through G-20 columns. From the absorbances at 496 nm of the S-1 eluents in 5 M urea and 50 mM Tris-HCl (pH 8.5), the moles of dye per mole of S-1 are calculated (upper curve). Some aliquots are further dialyzed before the absorbances (lower curve) are measured.

Reaction of S-1 with IAF. S-1 at 100 μM was mixed with 0.5 mM 5-IAF [20 mM 5-IAF dissolved in 100% *N*,*N*-dimethylformamide (DMF) was added] in 0.1 M KCl, 20 mM TES (pH 7.0), and 2 mM $MgSO_4$ at 0 °C. At various times, 0.8-mL aliquots were withdrawn and immediately mixed with 25 μL of 100 mM DTT to terminate the reaction. And then, in order to remove free dye, the aliquots were passed through G-20 Sephadex column equilibrated with buffer A. Half of each eluent was further dialyzed against buffer A for 24 h (the buffer solution was changed 3 times). The concentration of bound dye was estimated from the optical density ($E_{496} = 7.7 \times 10^4$ M^{-1} cm^{-1}) in 5 M urea and 50 mM Tris-HCl (pH 8.5) at 20 °C (Takashi, 1979). The protein concentration of labeled S-1 was estimated by the method of Lowry et al. (1951), from a calibration curve with unlabeled S-1 whose concentration had been determined from the 280-nm absorbance.

Labeled S-1 used below was obtained by incubating S-1 with 5-IAF for 45–60 min under the same conditions as above and removing free dye by means of the G-20 column and extensive dialysis. S-1 labeled with 6-IAF was also obtained by using the same procedure as that for 5-IAF-S-1. Hereafter, we use $S\text{-}1_\alpha$* (α = 5 or 6) to denote 5-IAF-labeled or 6-IAF-labeled S-1.

Fluorescence Measurements. Steady-state fluorescence and light scattering measurements were made with a Hitachi Perkin-Elmer fluorometer MPF-4 thermostated at 22 °C. Fluorescence lifetime measurements were made with a single-photon counting lifetime instrument.

Stopped-Flow Studies. A Durrum D-117 stopped-flow spectrophotometer thermostated at 22 °C was used for kinetic studies of acto–$S\text{-}1_5$*–nucleotide interactions. In the fluorescence mode, excitation at 498 nm was used, and emission at 550 nm (with an interference filter) was observed. In the light scattering mode, excitation light at 345 nm was used, and scattered light at 345 nm (with an interference filter) was observed.

Results

Reaction of S-1 with 5-IAF. 5-IAF that had not covalently bound to S-1 was removed from the S-1 plus 5-IAF mixture in two steps, first by filtration through a G-20 Sephadex column and then by dialysis. As shown with open circles in Figure 1, just after passage through the G-20 column the

[1] Abbreviations: 5-IAF, 5-(iodoacetamido)fluorescein; S-1, myosin subfragment 1; ε-ATP, 1,N^6-ethenoadenosine 5′-triphosphate; DMF, *N*,*N*-dimethylformamide; $S\text{-}1_5$*, 5-IAF-labeled S-1; $S\text{-}1_6$*, 6-IAF-labeled S-1; PP_i, pyrophosphate; 5-IAF-Cys, compound of 5-IAF reacted with *N*-acetylcysteine; IAA, iodoacetamide; 1,5-IAEDANS, *N*-(iodoacetyl)-*N*′-(5-sulfo-1-naphthyl)ethylenediamine; TES, 2-[[tris(hydroxymethyl)methyl]amino]ethanesulfonic acid; Tris, tris(hydroxymethyl)-aminomethane; EDTA, ethylenediaminetetraacetic acid.

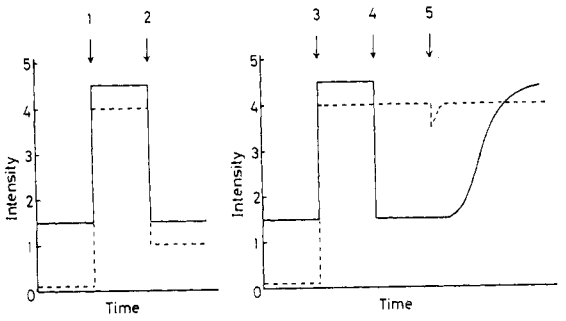

FIGURE 2: Fluorescence changes in S-1_5* induced by F-actin and nucleotides. The fluorescence (indicated by solid lines) was measured at 520 nm when excited at 330 nm. The light scattering (indicated by broken lines) was measured at 400 nm. At the marks of arrows 1 and 3, F-actin (10 μM) was added to 4 μM S-1_5* in buffer A [20 mM KCl, 10 mM TES (pH 7.5), and 2 mM $MgSO_4$] at 22 °C. At the marks of arrows 2 and 4, 0.14 mM ATP or ADP was added to the acto–S-1_5*, respectively. At the mark of arrow 5, 20 μg/mL myokinase, 10 μg/mL hexokinase, and 10 mM glucose were added together into the acto–S-1_5*–ADP solution.

number (N) of 5-IAF molecules bound per S-1 molecule as a function of time showed fast and slow phases, although the filtration yielded exactly two bands of 5-IAF yellow color. The extrapolation of the slow phase intercepted the y axis at N = 1. This slow phase, however, disappeared after the samples were dialyzed, and N then became saturated at N = 1. Therefore, on S-1 there is/are unspecific, noncovalent binding site(s) for 5-IAF [probably a hydrophobic pocket(s)] in addition to the specific site of covalent attachment The specific site was identified to be the SH_1 group, judging from changes that its reaction causes in the EDTA- and Ca^{2+}-ATPase activities (the data are now shown).

*Effects of Nucleotides and F-Actin on Fluorescence of S-1_5**. Formation of complexes of S-1_5* with Mg^{2+}-ADP, Mg^{2+}-ATP, or Mg^{2+}-PP_i did not change the fluorescence of S-1_5*. Formation of the rigor complex, in the absence of even a trace amount of nucleotides is, however, accompanied by a 3-fold (or a little more) increase in the fluorescence intensity and by a slight red shift (about 2 nm) of the excitation maximum (see Figures 2 and 3). Figure 2 shows that, on addition of Mg^{2+}-ATP to acto–S-1_5*, the light scattering at 400 nm indicated complete dissociation of S-1_5* from F-actin and that the increment in fluorescence disappeared; however, on addition of Mg^{2+}-ADP, the light scattering indicated little dissociation, but the fluorescence increment again disappeared. In order to examine for the reversibility of the fluorescence changes induced by F-actin and Mg^{2+}-ADP, hexokinase, myokinase, and glucose were added together to the acto–S-1_5*-ADP solution in order to convert all the ADP into inert AMP [of course, transiently, a little ATP is produced from ADP (via myokinase), but eventually all nucleotides convert to AMP]. The light scattering dropped a little due to production of ATP and then immediately recovered to the previous level, while the fluorescence intensity, after an initial lag-phase, gradually increased, approaching the level of the rigor complex. In summary, the fluorescence signal is low in M, M–N, and A–M–ADP but high in A–M (herein, M = S-1_5*, N = ATP, ADP, or PP_i, A = actin).

To study the mechanism of the large enhancement in the fluorescence intensity, the effect of F-actin on the fluorescence lifetime and absorbance of S-1_5* was measured. Surprisingly, neither parameter was changed by adding F-actin (the lifetime was about 4.0 ns). How is the large enhancement in fluorescence intensity possible without any changes in the lifetime or in absorption? The only possible explanation seems to be that the attached fluorescein is statically quenched by

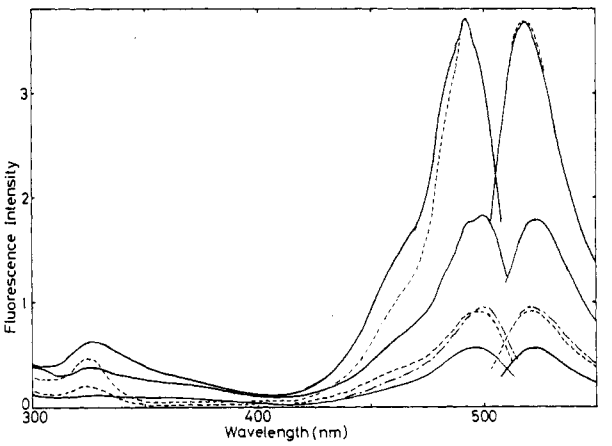

FIGURE 3: Excitation (left branch) and emission (right branch) spectra of S-1_α* (α = 5 or 6) treated in various ways. Solid lines are for α = 5, and broken lines are for α = 6. (Bottom of solid lines) S-1_5* (4 μM) alone; (middle of solid lines) acto–S-1_5* (10 μM F-actin plus 4 μM S-1_5*); (top of solid lines) extensively digested S-1_5* with trypsin; (bottom of broken lines) S-1_6* (4 μM) alone; (top of broken lines) extensively digested S-1_6* with trypsin; (–·–) acto–S-1_6*. Digestion of S-1_α* (4 μM) was carried out in buffer A at 22 °C for 60 min with a 2 times weight excess of trypsin over S-1_α*. During the digestion, the fluorescence intensity was gradually increased and saturated in about 45 min.

some amino acid residue located near the SH_1 group and that binding of F-actin to S-1_5* withdraws the fluorescein, resulting in a large increase in the fluorescence intensity (static quenching of fluorescence is not accompanied by changes in lifetime or absorption). If this explanation is correct, the fluorescence intensity must increase upon removing the quenching amino acid. This can be accomplished by destroying the S-1_5* structure. As shown by the top curves in Figure 3, extensive digestion of S-1_5* with trypsin was accompanied by a large increase (ca. 6.6-fold) in the fluorescence intensity (but, little change in the lifetime) and by blue shifts of the excitation and emission maxima. The spectra of digested S-1_5* were almost identical with that of free 5-IAF–*N*-acetylcysteine conjugate (5-IAF-Cys).

It is of interest to see if the F-actin effect observed with S-1_5* might also be observed with S-1_6* wherein the fluorescein is buried in S-1 in a steric arrangement different from that in S-1_5*. As shown in Figure 3, the binding of F-actin to S-1_6* increased the fluorescence of S-1_6* very little, but a slight red shift of the excitation maximum was again observed. Tryptic digestion of S-1_6*, however, also induced a large fluorescence increase (about 4-fold), implying that 6-IAF also suffers static quenching, but binding of F-actin apparently cannot take the quencher amino acid away from the fluorescein.

Titration of S-1_5 with F-Actin.* As studied above, the fluorescence signal of S-1_5* can distinguish the rigor state from the other states. Therefore, this fluorescence signal allows us to measure spectroscopically several kinetic parameters of actin–myosin–nucleotide interactions.

First, S-1_5* was titrated with F-actin by monitoring the fluorescence increment, in order to obtain the association constant of S-1_5* for F-actin. As shown by open circles in Figure 4, the titration did not give a hyperbolic curve but a slight sigmoidal one. This could be due to a small amount of contamination of unlabeled S-1 in the S-1_5* sample, assuming a weaker affinity of S-1_5* for F-actin than unlabeled S-1. Actually, the S-1_5* sample contained about 5% of unlabeled S-1. In order to test this possibility, S-1_5* was again titrated with F-actin in the presence of various amounts of unlabeled S-1 (1.1, 2.1, or 3.1 μM), keeping the total concentration of

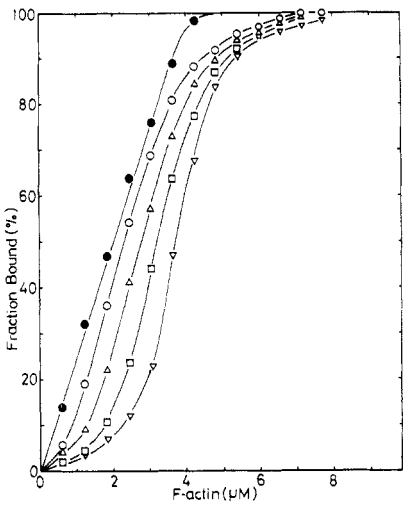

FIGURE 4: Titration of S-1_5* with F-actin in the presence of unlabeled S-1. 5 μL of 246 μM F-actin was successively added to 2 mL of 4 μM S-1_5* plus S-1 in buffer A at 22 °C. The fraction of bound S-1_5* was estimated from the changes in the fluorescence at 520 nm (when excited at 330 nm). (○) 3.8 μM S-1_5* plus 0.2 μM S-1; (△) 2.9 μM S-1_5* plus 1.1 μM S-1; (□) 1.9 μM S-1_5* plus 2.1 μM S-1; (▽) 0.9 μM S-1_5* plus 3.1 μM S-1. The closed circles are of titration of unlabeled S-1 (4 μM) measured by the light scattering at 400 nm in buffer A at 22 °C.

S-1_5* plus S-1 constant (4 μM). As can be seen in Figure 4, the titration curve was shifted to the right side by increasing the fraction of unlabeled S-1. So, now there is no doubt that introduction of 5-IAF to the SH_1 group reduces the affinity of S-1 for F-actin. It is easy to estimate the extent of the affinity reduction from a simple calculation and the titration data. Setting K and K' as the association constants of unlabeled and labeled S-1, respectively, $\rho = K/K'$, and A_0 as the added actin concentration at which half of the S-1_5* binds to F-actin, we find that

$$A_0 = (1/2)C + 1/K' + \frac{\rho - 1}{2(1 + \rho)}M_0 \qquad (1)$$

where M_0 and C are total concentrations of unlabeled S-1 and unlabeled S-1 plus S-1_5*, respectively. From the data in Figure 4 and eq 1, ρ and K' were estimated to be 50 and 4.8 × 10^6 M^{-1}, respectively. The association constant of unlabeled S-1, 2.4 × 10^8 M^{-1}, seems to be greater than those reported before, 2 × 10^7 M^{-1} in 0.1 M KCl (White & Taylor, 1976) and 5 × 10^6 M^{-1} in 0.2 M KCl (Greene & Eisenberg, 1980). But, considering the ionic strength dependence of the association constant (Highsmith, 1978), our value obtained in 20 mM KCl is of a reasonable order.

Titration of Acto–S-1_5 with Mg^{2+}-ADP and Mg^{2+}-PP_i.* Second, the fluorescence signal from S-1_5* was utilized to obtain the dissociation constant of Mg^{2+}-ADP for acto–S-1_5*. Aliquots of 5 μL of Mg^{2+}-ADP solution were successively added to 2 mL of acto–S-1_5* (10 μM F-actin plus 4 μM S-1_5*) in a fluorescence cuvette while the fluorescence was monitored at 520 nm (excitation at 330 or 460 nm) and the light scattering at 400 nm. As shown in Figure 5, the light scattering indicated no dissociation, while the fluorescence signal gradually decreased, the half-drop being at 2.5 μM Mg^{2+}-ADP added. Because there is no dissociated S-1_5* in the solution, 2 μM acto–S-1_5* is fully occupied by Mg^{2+}-ADP at 2.5 μM Mg^{2+}-ADP added. Therefore, the dissociation constant of Mg^{2+}-ADP, K_d, is estimated to be 0.5 μM.

Next, Mg^{2+}-PP_i (5 μL) was successively added to 2 mL of acto–S-1_5*. As shown in Figure 6, both light scattering and fluorescence decreased with increasing Mg^{2+}-PP_i concentration. Both of these decay curves had two distinctive phases, i.e., a "fast" and then a "slow" phase. Furthermore, the two decay curves did not coincide exactly. As shown in the insert of Figure 6, the change in the fluorescence signal always preceded that in light scattering, whcih seems to imply that the fluorescence signal from the ternary complex, acto–S-1_5*–PP_i, may be as low as that from acto–S-1_5*–ADP. The curve of ΔF vs. ΔLS had a saddle point at about 50% of ΔLS, which corresponds to the junction of the fast and slow phases mentioned above. Therefore Mg^{2+}-PP_i appears to have two different association constants for acto–S-1_5* (roughly esti-

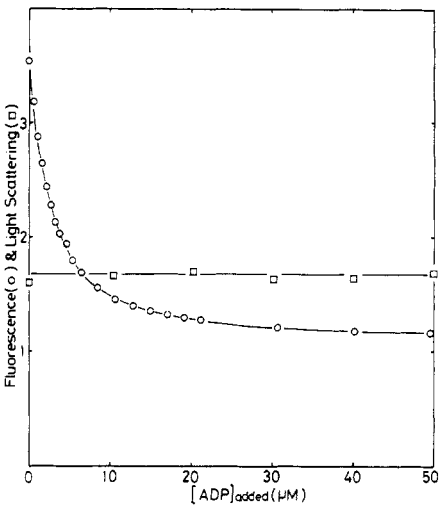

FIGURE 5: Titration of acto–S-1_5* with Mg^{2+}-ADP. 5 μL of Mg^{2+}-ADP was successively added to 2 mL of acto–S-1_5* (10 μM F-actin plus 4 μM S-1_5*) in buffer A at 22 °C. The fluorescence (○) was measured at 520 nm when excited at 330 nm, and the light scattering (□) was measured at 400 nm.

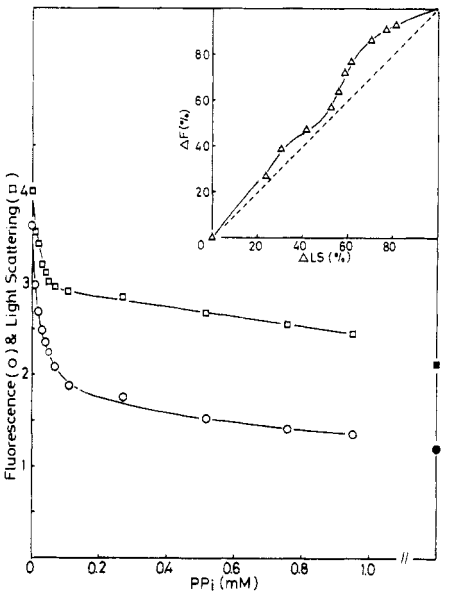

FIGURE 6: Binding of Mg^{2+}-PP_i to acto–S-1_5*. Conditions are the same as those of Figure 5 except that PP_i was used. (○) Fluorescence intensity; (□) light scattering intensity. In contrast to the Mg^{2+}-ADP case (Figure 5), PP_i dissociates the acto–S-1_5* complex. To get complete dissociation, 0.1 mM of Mg^{2+}-ATP was added [(●) fluorescence; (■) light scattering]. The inserted figure shows percent fraction of the fluorescence intensity change (ΔF) as a function of percent fraction of light scattering change (ΔLS). If the quantum yield of fluoresecence from the ternary complex, q(A–M–PP_i), is the same as that from acto–S-1_5*, q(A–M), ΔF should be directly proportional to ΔLS. So, the inserted figure indicates that q(A–M–PP_i) is much lower than q(A–M). The difference between the solid line and the broken line in the inserted figure equals the percent fraction of the ternary complex provided that q(A–M–PP_i) is equal to q(M).

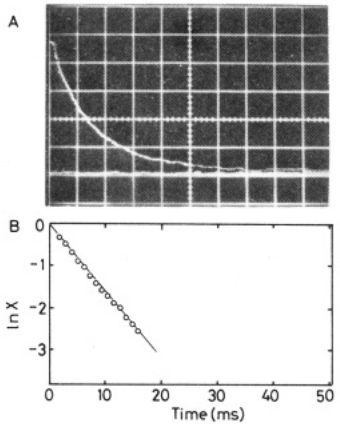

FIGURE 7: (A) Memory oscilloscope trace of fluorescence change after mixing Mg^{2+}-ADP with acto-S-1_5*. The fluorescence was monitored at 550 nm when excited at 498 nm. 28 μM ADP in buffer A was quickly mixed with the same volume of acto-S-1_5* (20 μM F-actin plus 3 μM S-1_5*) in buffer A at 22 °C. x–y scales are 5 ms/division and 0.1 V/division, respectively. (B) Semilog plots of the above trace.

mated, 8×10^4 M^{-1} and 1.4×10^3 M^{-1}). This may bear on an observation made by Nauss et al. (1969). They observed that myosin bound 2 mol of $PP_i/5 \times 10^5$ g of myosin with an association constant of 2.07×10^6 M^{-1}, while natural acto-myosin bound only 1 mol of $PP_i/5 \times 10^5$ g of myosin with an association constant of 5.6×10^5 M^{-1}.

Stopped-Flow Studies. Finally, the fluorescence signal of S-1_5* was employed in kinetic studies on the interaction of acto-S-1_5* with nucleotides to obtain rate constants relevant to the interaction. The rate constants of nucleotide binding to acto-S-1 have never been directly measured before, for lack of a signal sensitive to the processes [although the ϵ-ATP fluorescence signal in an acrylamide solution can distinguish free and bound ϵ-ATP, the signal is not sensitive to the initial binding step but to a subsequent isomerization step (Ando et al., 1982b; Ando & Duke, 1983)].

Figure 7A shows the trace of fluorescence intensity change when 14 μM (final) Mg^{2+}-ADP was quickly mixed with acto-S-1_5* (10 μM F-actin plus 1.5 μM S-1_5*). The semilog plots of this fluorescence transient produced a fairly straight line whose slope (see Figure 7B) gives the rate of binding. The rate of fluorescence change as a function of ADP concentration is shown in Figure 8. The extrapolation of the linear plot has an intercept on the ordinate. Although it is difficult to determine the intercept exactly, it definitely lies between 0 and 10^{-1} s. The rate of fluorescence decrease equals $k_- + k$[ADP] if $[\text{acto-S-}1_5^*]_{\text{total}} << [\text{ADP}]$ in a simple binding scheme:

$$\text{acto-S-}1_5^* + \text{ADP} \underset{k_-}{\overset{k}{\rightleftharpoons}} \text{acto-S-}1_5^*\text{-ADP}$$

Therefore, k_- and k can be estimated from the intercept and the slope, respectively, of the linear plot in Figure 8: this results in $k_- = 0$–10 s^{-1} and $k = 10^7$ s^{-1} M^{-1}. k_- can be also estimated by using the k value and the dissociation constant, 0.5 μM, of Mg^{2+}-ADP obtained in the previous section. A simple calculation gives $k_- = 5$ s^{-1}, which agrees with the result of the first calculation.

After Mg^{2+}-ATP was quickly mixed with acto-S-1_5* (10 μM F-actin plus 1.0 μM S-1_5*), both the fluorescence and light scattering intensities decayed with time in single-exponential manners (the data are not shown). The rates of decrease in fluorescence and in light scattering as a function of ATP concentration are shown in Figure 8. Clearly, the rate of fluorescence change, k_F, is directly proportional to the ATP concentration. On the other hand, comparable linearity is not

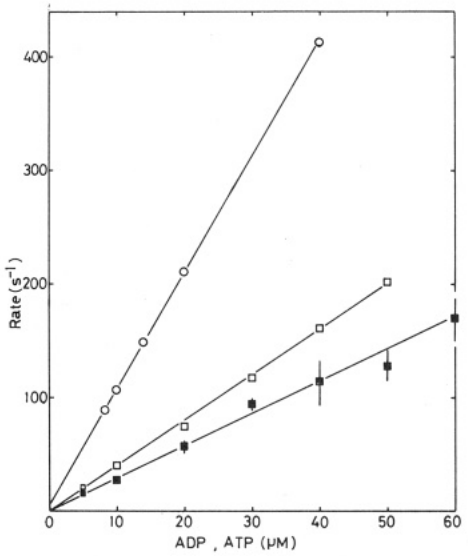

FIGURE 8: Dependence on nucleotide concentration of the rate of fluorescence and light scattering changes after nucleotide was quickly mixed with acto-S-1_5*: (○) rate of fluorescence change with Mg^{2+}-ADP; (□) rate of fluorescence change with Mg^{2+}-ATP; (■) rate of light scattering change with Mg^{2+}-ATP. The vertical bars of (■) plots indicate scatters of three to four data.

obtained with the rate of light scattering change, k_{LS}, because of experimental error. It seems sure, however, that k_F is always greater than k_{LS} at every ATP concentration; i.e., ATP binding precedes acto-S-1_5* dissociation. By employing a simple scheme of acto-S-1_5* dissociation by ATP, i.e.

$$\text{acto-S-}1_5^* + \text{ATP} \underset{k_{-1}}{\overset{k_1}{\rightleftharpoons}} \text{acto-S-}1_5^*\text{-ATP} \xrightarrow{k_2} \text{actin} + \text{S-}1_5^*\text{-ATP}$$

k_F is nearly equal to k_1[ATP]. The second-order rate constant, k_1, is estimated to be 4×10^6 s^{-1} M^{-1}. At infinite concentration of ATP, k_{LS} should saturate and become k_2. Since k_{LS} does not appear to be approaching saturation (within experimental error and with the ATP concentration used), k_2 must be much greater than 200 s^{-1}, which agrees with Lymn & Taylor (1971) and Finlayson et al. (1969). It may be worth noting that the second-order rate constant for binding is a little greater for Mg^{2+}-ADP than for Mg^{2+}-ATP.

Discussion

The reduction in the quantum yield of 5-IAF attached to the SH_1 of S-1 relative to free 5-IAF-Cys is about 85%. But, the lifetime and the absorption of the two species are nearly identical, except for slight differences in the excitation and emission maxima. A similar observation has been reported before; the fluorescence of fluorescein is extensively quenched (~90%) when the fluorophore binds to rabbit anti-fluorescyl IgG antibody (Watt & Voss, 1977). Screening of individual amino acids for their ability to quench the fluorescence of free fluorescein indicated that Trp, Tyr, and Met are quenchers with effectiveness in that order and that the quenching by Trp possesses both static and dynamic components (Watt & Voss, 1977). Since freedom of movement of fluorescein and quencher amino acid is restricted within protein, static quenching must be predominant in our observation. Although at present we cannot identify the particular amino acid, it may be worth considering the amino acid sequence around SH_1 (Tong & Elzinga, 1983). Within 40 amino acids located around SH_1 there are two Tyr and one Met. Trp does not exist in the 20K fragment of S-1. The nearest Trp is located in the 20K–50K junction.

The quantum yield of fluorescence from acto–S-1_5* is still about 50% lower than that of free 5-IAF-Cys. That is, the actin-induced conformational change in S-1 cannot take the quencher completely away from the attached fluorescein. It is unlikely that there are two kinds of acto–S-1_5* (one in which fluorescein is always quenched and one in which fluorescein is always unquenched). It is more likely that between fluorescein and quencher there exists some contact equilibrium that is modulated by actin-induced or nucleotide-induced conformational changes. It is of interest that Mg^{2+}-ADP binding to acto–S-1_5* cancels the actin-induced conformational change around the attached fluorescein. So, actin-binding and nucleotide-binding sites on S-1 communicate through a region where fluorescein is located (Morales et al., 1982). And also, the present results suggest that actin-bound S-1 can exist in at least two different conformational states depending on the presence of Mg^{2+}-ADP. Actually, Borejdo et al. (1982) showed that rhodamine-labeled S-1 assumes different orientational states with respect to the F-actin axis when bound to it in rigor or when bound in the presence of Mg^{2+}-ADP. The transition between these states may be important in the process of tension generation.

We have demonstrated how conveniently kinetic parameters of acto–S-1–nucleotides interactions can be obtained by utilizing the fluorescence signal of 5-IAF attached to S-1. Of course, chemical modification of protein alters its structure and function. It is already well-known that SH_1 modification with SH-directed reagents such as iodoacetamide (IAA), *N*-(iodoacetyl)-*N'*-(5-sulfo-1-naphthyl)ethylenediamine (1,5-IAEDANS), *N*-ethylmaleimide, or a spin label, *N*-(2,2,6,6-tetramethyl-4-piperidinyl-1-oxy)iodoacetamide, reduces the maximum actin-activated S-1 or heavy meromyosin ATPase activities and also changes the kinetic parameters (Mulhern & Eisenberg, 1978; Takashi, 1979; Sleep et al., 1981). In the present study, it was shown that a relatively large reduction ($\sim 1/50$) of the affinity of S-1 for actin is induced by labeling the SH_1 with 5-IAF. SH_1 labeling with other reagents, i.e., 1,5-IAEDANS or IAA, does not cause a large reduction of S-1 affinity for F-actin (Highsmith et al., 1976; Mulhern & Eisenberg, 1978). Actually, when IAA-S-1 was used instead of unlabeled S-1 in the titration experiment shown in Figure 4, the shifts of the titration curve were nearly the same as those with unlabeled S-1, implying that the affinity of IAA-S-1 is the same as that of unlabeled S-1. Moreover, treatment of S-1 with 5% DMF, which has been used as a solvent for 5-IAF, did not cause any change in S-1. The relatively large affinity reduction caused by reaction with 5-IAF is probably due to the relatively large size of the fluorescein molecule or due to its hydrophobicity.

From the fluorescence change of acto–S-1_5* induced by Mg^{2+}-ADP, the dissociation constant of Mg^{2+}-ADP for acto–S-1 was estimated to be 0.5 μM. This value is quite low, compared with values reported for rabbit skeletal acto–S-1 of 200 μM (White, 1977), 143 μM (Greene & Eisenberg, 1980), and 37 μM (Highsmith, 1976). The rate of Mg^{2+}-ADP dissociation from rabbit skeletal acto–S-1 has been estimated to be faster than 10^3 s^{-1} (White, 1977) by measuring the rate of dissociation of acto–S-1 by Mg^2-ATP in the presence of Mg^{2+}-ADP. Therefore, our low estimate of the dissociation constant, 0.5 μM, is due to a low rate of dissociation (i.e., 5 s^{-1}). The rate of Mg^{2+}-ADP association, 10^7 s^{-1} M^{-1}, agrees with the estimate ($>5 \times 10^6$ s^{-1} M^{-1}) made by White (1977).

Although the enzymatic properties of S-1 are modified by introducing fluorescein to the SH_1, application of the fluorescence signal to studies in vivo (as well as in vitro) may be fruitful. Muscle fibers whose cross-bridges are labeled with 1,5-IAEDANS or 5-IAF can still generate tension (Nihei et al., 1974; Borejdo et al., 1979). The fluorescence dichroism of labeled fibers responds to nucleotide occupation of cross-bridges (Borejdo et al., 1982). It will be of interest to see whether the transients of fluorescein signal as a chemical signal correlate with the tension transients induced by quick stretch of the isometrically contracting fibers or by flash photolysis of caged ATP.

Acknowledgments

I thank Dr. P. Torgerson for the lifetime measurements and Professor M. F. Morales for helpful discussion, encouragement, support, and critical reading of the manuscript. I also thank Drs. R. Takashi and G. Weber for useful suggestions.

Registry No. Mg^{2+}-ADP, 7384-99-8; Mg^{2+}-PP_i, 13446-24-7; Mg^{2+}-ATP, 1476-84-2; 5-(iodoacetamido)fluorescein, 63368-54-7.

References

Ando, T., & Asai, H. (1979) *J. Mol. Biol. 129*, 265–278.
Ando, T., & Duke, J. A. (1983) *Biochem. Biophys. Res. Commun. 115*, 312–316.
Ando, T., Duke, J. A., Tonomura, Y., & Morales, M. F. (1982a) *Biochem. Biophys. Res. Commun. 109*, 1–6.
Ando, T., Duke, J. A., Tonomura, Y., & Morales, M. F. (1982b) *Biophys. J. 37*, 46a.
Borejdo, J., Putnam, S. V., & Morales, M. F. (1979) *Proc. Natl. Acad. Sci. U.S.A. 76*, 6346–6350.
Borejdo, J., Assulin, O., Ando, T., & Putnam, S. (1982) *J. Mol. Biol. 158*, 391–414.
Finlayson, B., Lymn, R. W., & Taylor, E. W. (1969) *Biochemistry 8*, 811–819.
Goldman, Y. E., Hibberd, M. G., McCray, J. A., & Trentham, D. R. (1982) *Nature (London) 300*, 701–705.
Greene, L. E., & Eisenberg, E. (1980) *J. Biol. Chem. 255*, 543–548.
Highsmith, S. (1976) *J. Biol. Chem. 251*, 6170–6172.
Highsmith, S. (1978) *Biochemistry 17*, 22–26.
Highsmith, S., Mendelson, R. A., & Morales, M. F. (1976) *Proc. Natl. Acad. Sci. U.S.A. 73*, 133–137.
Huxley, A. F., & Simmons, R. M. (1971) *Nature (London) 233*, 533–538.
Huxley, A. F., & Simmons, R. M. (1973) *Cold Spring Harbor Symp. Quant. Biol. 37*, 669–680.
Lowry, H., Rosebrough, N. J., Farr, A. L., & Randall, R. J. (1951) *J. Biol. Chem. 193*, 265–275.
Lymn, R. W., & Taylor, E. W. (1971) *Biochemistry 10*, 4617–4624.
Morales, M. F. (1982) *Proc. Natl. Acad. Sci. U.S.A. 79*, 1126–1128.
Morales, M. F., Borejdo, J., Botts, J., Cooke, R., Mendelson, R. A., & Takashi, R. (1982) *Annu. Rev. Phys. Chem. 33*, 319–351.
Mulhern, S. A., & Eisenberg, E. (1978) *Biochemistry 17*, 4419–4425.
Nauss, K. M., Kitagawa, S., & Gergely, J. (1969) *J. Biol. Chem. 244*, 755–765.
Nihei, T., Mendelson, R. A., & Botts, J. (1974) *Biophys. J. 14*, 236–242.
Sleep, J. A., Trybus, K. M., Johnson, K. A., & Taylor, E. W. (1981) *J. Muscle Res. Cell Motil. 2*, 373–399.
Spudich, J. A., & Watt, S. (1971) *J. Biol. Chem. 246*, 4866–4871.

Takashi, R. (1979) *Biochemistry 18*, 5164–5169.
Tong, S. W., & Elzinga, M. (1983) *Fed. Proc., Fed. Am. Soc. Exp. Biol. 42*, 2211.
Tonomura, Y., Appel, P., & Morales, M. F. (1966) *Biochemistry 5*, 515–521.
Watt, R. M., & Voss, E. W., Jr. (1977) *Immunochemistry 14*, 533–541.
Weeds, A. G., & Taylor, R. S. (1975) *Nature (London) 257*, 54–56.
White, H. D. (1977) *Biophys. J. 17*, 40a.
White, H. D., & Taylor, E. W. (1976) *Biochemistry 15*, 5818–5826.

Crystals of *Bacillus stearothermophilus* Tryptophanyl-tRNA Synthetase Containing Enzymatically Formed Acyl Transfer Product Tryptophanyl-ATP, an Active Site Marker for the 3′ CCA Terminus of Tryptophanyl-tRNA^{Trp} †

David E. Coleman and Charles W. Carter, Jr.*

ABSTRACT: It has previously been shown that tryptophanyl-tRNA synthetase from *Bacillus stearothermophilus* crystallizes in different forms, depending on the substrates present during crystallization [Carter, C. W., Jr., & Carter, C. W. (1979) *J. Biol. Chem. 254*, 12219–12223]. Radiolabeling experiments show that the tetragonal crystals (type IV), grown in the presence of tryptophan and ATP, contain enzymatically formed 3′(2′)-tryptophanyladenosine 5′-triphosphate (Trp-ATP). Trp-ATP is formed by acyl transfer of the tryptophanyl moiety of an acyladenylate intermediate, Trp-5′-AMP, to a second molecule of ATP bound in the site normally occupied by the 3′ CCA terminus of tRNA^{Trp}. This compound is therefore a chemical marker in type IV crystals for that part of the tRNA binding site on the synthetase. Solution of this crystal structure, now in progress, may therefore provide useful information concerning the mechanism of aminoacylation of tRNA^{Trp} by this enzyme and may help locate its tRNA binding site.

Tryptophanyl-tRNA synthetase catalyzes production of tryptophanyl-tRNA^{Trp} from tryptophan, ATP, and tRNA^{Trp}. Since the enzymes from both *Escherichia coli* (Muench, 1969) and *Bacillus stearothermophilus* (Atkinson et al., 1979) catalyze tryptophan-dependent [^{32}P]pyrophosphate exchange, it is reasonable to assume that aminoacylation normally proceeds via the conventional, two-step reaction (Scheme I). In reaction 1 the α-phosphate of ATP undergoes nucleophilic attack by the carboxyl group of tryptophan to form the adenylate, tryptophanyl-5′-AMP (Trp-AMP).[1] The second reaction (2) involves transfer of the aminoacyl moiety to the 2′- or 3′-hydroxyl group of the ribose moiety on the terminal adenosine of tRNA^{Trp}. We showed previously (Carter & Carter, 1979) that the tryptophanyl-tRNA synthetase from *B. stearothermophilus* can be crystallized in the presence of tryptophan and ATP. The actual ligands associated with this crystal form (type IV) are a matter of considerable interest because of the possibility that the crystals might contain a bound, enzymatically formed ligand.

Two different products can be envisioned for this enzyme in the presence of tryptophan and ATP. Since confusion may arise due to the superficial similarity between the two compounds, it is useful to describe them explicitly. One possibility is that the enzyme makes and binds the acyladenylate intermediate, Trp-5′-AMP (reaction 1 in Scheme I above). The other possibility is that the enzyme also carries out reaction 2 in Scheme I by using a second molecule of ATP as an acyl-group acceptor, synthesizing, and retaining the 3′(2′)-tryptophan ester of adenosine triphosphate (Trp-ATP). This second possibility is raised by previous studies of the tryptophan enzymes from beef pancreas (Weiss et al., 1959) and *E. coli* (Joseph & Muench, 1971b) in which ATP, at high concentrations, was found to serve as an acyl-group acceptor in place of the 3′-terminal adenosine of tRNA^{Trp} in reaction 2 of Scheme I.

Scheme I

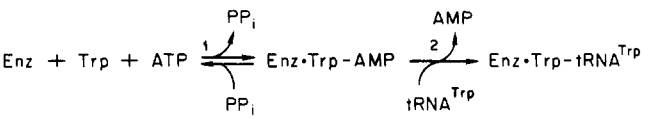

We report here that the tryptophan enzyme from *B. stearothermophilus* also produces Trp-ATP in solution and, further, that this compound is the major ligand bound to fresh type IV crystals. The structure and mode of synthesis of this compound imply that it is a product analogue, resembling the 3′ CCA terminus of Trp-tRNA^{Trp}, and that it therefore serves as a marker for the binding site of this end of tRNA^{Trp} on the synthetase. The mode of binding of Trp-ATP to type IV crystals can aid in elucidating the reaction mechanism of

† From the Departments of Biochemistry and Anatomy, University of North Carolina at Chapel Hill, Chapel Hill, North Carolina 27514. *Received May 23, 1983.* This work was supported by NIH Research Grant GM26203 and by American Cancer Society Institutional Grant IN-15X.

* Address correspondence to this author at the Department of Biochemistry.

[1] Abbreviations: Trp-ATP, 3′(2′)-tryptophanyladenosine 5′-triphosphate; Trp-AMP, tryptophanyl-5′-AMP; EDTA, ethylenediaminetetraacetate sodium salt; TLC, thin-layer chromatography; PEI, poly(ethylenimine); Bicine, *N,N*-bis(2-hydroxyethyl)glycine.

0006-2960/84/0423-0381$01.50/0